Structure, Vol. 12, 1967–1975, November, 2004, ©2004 Elsevier Ltd. All rights reserved. DOI 10.1016/j.str.2004.09.004

Crystal Structure of PriB, a Component of the *Escherichia coli* Replication Restart Primosome

Matthew Lopper,[1] James M. Holton,[2] and James L. Keck[1,*]
[1]Department of Biomolecular Chemistry
University of Wisconsin Medical School
550 Medical Sciences Center
1300 University Avenue
Madison, Wisconsin 53706
[2]Physical Biosciences Division
Lawrence Berkeley National Laboratory
University of California, Berkeley
Berkeley, California 94720

Summary

Maintenance of genome stability following DNA damage requires origin-independent reinitiation of DNA replication at repaired replication forks. In *E. coli*, PriA, PriB, PriC, and DnaT play critical roles in recognizing repaired replication forks and reloading the replisome onto the template to reinitiate DNA replication. Here, we report the 2.0 Å resolution crystal structure of *E. coli* PriB, revealing a dimer that consists of a single structural domain formed by two oligonucleotide/oligosaccharide binding (OB) folds. Structural similarity of PriB to single-stranded DNA binding proteins reveals insights into its mechanisms of DNA binding. The structure further establishes a putative protein interaction surface that may contribute to the role of PriB in primosome assembly by facilitating interactions with PriA and DnaT. This is the first high-resolution structure of a protein involved in *oriC*-independent replisome loading and provides unique insight into mechanisms of replication restart in *E. coli*.

Introduction

Complete and faithful replication of the genome requires the ability of cells to respond to DNA damage. Under normal growth conditions, replication forks formed at the bacterial origin of replication, *oriC*, frequently encounter sites of DNA damage that can result in their inactivation (reviewed in Cox et al., 2000). These stalled replication forks must be efficiently repaired to allow replication of the genome to resume. Processes that reinitiate replication at repaired forks thus represent major housekeeping functions in bacteria that are essential for viability. Reloading DNA synthesis machinery onto repaired replication forks requires the combined activities of enzymes involved in DNA replication, recombination, and repair, thereby providing a link between these critical aspects of genome maintenance.

In *E. coli*, a number of proteins, collectively referred to as the primosome, are responsible for reactivating repaired replication forks. The *E. coli* primosome proteins were first identified as factors necessary for the in vitro conversion of bacteriophage ϕX174 single-stranded DNA (ssDNA) to its duplex replicative form (Schekman et al., 1975). Historically, this system provided a model for lagging strand DNA synthesis wherein the role of the primosome is to repeatedly synthesize short RNA oligonucleotides along the DNA template to prime Okazaki fragment synthesis. The seven proteins comprising the primosome, PriA, PriB, PriC, DnaT, DnaB, DnaC, and DnaG, were isolated biochemically based on this system (Schekman et al., 1975; Wickner and Hurwitz, 1974). Subsequently, it was shown that *E. coli* possesses two primosomes: one that catalyzes replisome assembly at the bacterial origin of replication (*oriC*) and involves three of the defined primosome proteins (DnaB, DnaC, and DnaG), and a second that initiates replication at the ϕX174 origin (primosome assembly site, *pas*) and involves all seven proteins. While DnaB (the replicative helicase), DnaC (the helicase loading protein), and DnaG (primase) were established as essential factors in chromosomal DNA replication initiating at *oriC*, the biological roles of PriA, PriB, PriC, and DnaT were less clear (Kaguni and Kornberg, 1984). Much progress has been made in recent years to elucidate the biological roles of the ϕX174 primosome proteins. It is now clear that PriA, PriB, PriC, and DnaT function to catalyze the reactivation of replication forks that have stalled at sites of DNA damage. These proteins have become collectively known as the replication restart primosome (Sandler and Marians, 2000).

E. coli primosome protein B (PriB) was originally identified as one of several factors comprising "protein n," an N-ethylmaleimide-sensitive protein complex required to support replication of ϕX174 ssDNA (Low et al., 1982). The gene encoding PriB protein appears to have arisen by duplication of the gene encoding single-stranded DNA binding protein (SSB) with subsequent evolution that led to its specialized function in replication (Ponomarev et al., 2003; Zavitz et al., 1991). Despite their proposed common lineage, *E. coli* PriB and SSB have limited amino acid sequence similarity (Figure 1A). Furthermore, the *priB* gene is not well conserved among sequenced bacterial genomes as homologs have been identified only in the β- and γ-subdivisions of proteobacteria (Ponomarev et al., 2003). At present, no *priB* homologs have been identified in eukaryotic genomes. While it is likely that most organisms have a requirement for restarting repaired replication forks following DNA damage, it is not yet clear if a PriB-like activity is uniformly utilized.

The function of PriB in the bacterial replication restart primosome is not well understood at the molecular level. PriB physically interacts with SSB and binds naked ssDNA or SSB-coated ssDNA in vitro (Allen and Kornberg, 1993; Low et al., 1982). It is thought that PriB assembles into the primosome following binding of PriA to the appropriate DNA substrate, such as a D-loop recombination intermediate, after which PriB assists in recruiting DnaT into the primosomal complex (Liu et al., 1996; Liu and Marians, 1999; Ng and Marians, 1996).

*Correspondence: jlkeck@wisc.edu

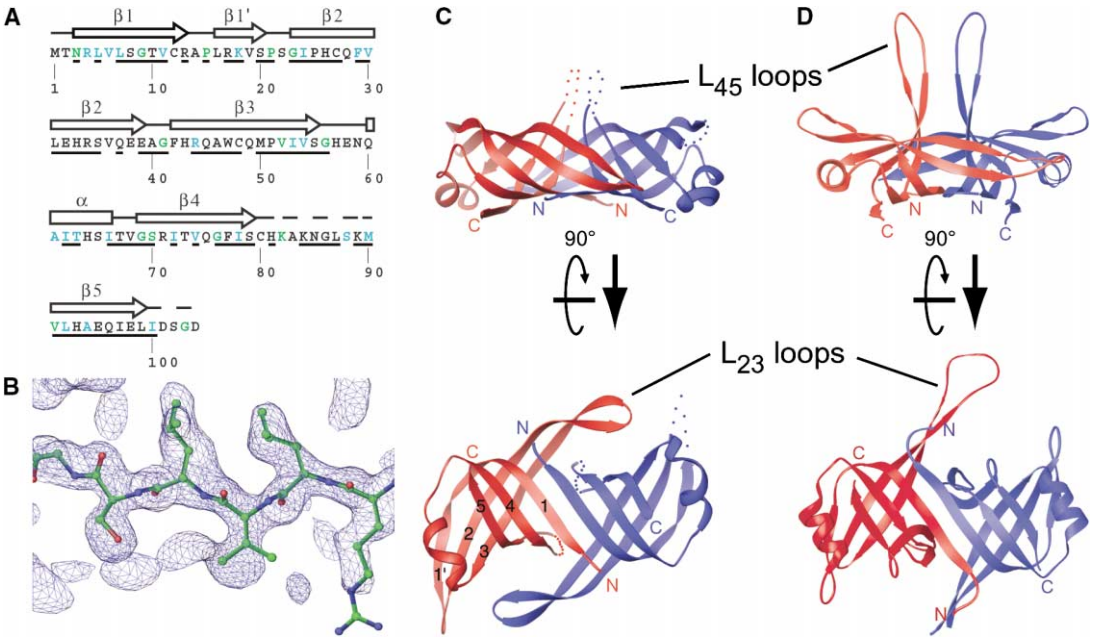

Figure 1. Structure of *E. coli* PriB

(A) Secondary structural elements of PriB are shown above the corresponding residues in the primary sequence, which is colored to indicate residues that are highly similar (teal) or identical (green) to *E. coli* SSB. Underlined residues are well conserved among 16 bacterial PriB family members. Dashed lines indicate regions of the primary sequence absent from the model due to lack of electron density.

(B) Representative solvent-flattened experimental electron-density map at 2.0 Å resolution contoured at 1.3 σ above the mean, rendered with the program RIBBONS (Carson, 1997). The stick model overlaying the electron density is that of the refined PriB model and is colored according to atom type with carbon atoms in green, oxygen atoms in red, and nitrogen atoms in blue.

(C) Orthogonal views of a ribbon diagram of the crystal structure of PriB. Chain A is colored red and chain B is colored blue. Individual β strands in chain A are numbered as in (A). Dotted lines represent regions of the protein that are absent from the model.

(D) Orthogonal views of a ribbon diagram of the crystal structure of *E. coli* SSB (Raghunathan et al., 2000). Only two molecules of the SSB tetramer are rendered and they are colored as in (C). Ribbon diagrams were rendered with the program RIBBONS (Carson, 1997).

The complex of PriA, PriB, and DnaT may represent the minimal machinery necessary to recruit the replicative helicase, DnaB, and helicase loading protein, DnaC, to the site of primosome assembly. DnaB unwinds duplex DNA and recruits the final component of the primosome, DnaG primase.

Deletions of *priB* in *E. coli* have essentially wild-type phenotypes, an observation that conflicts with the supposed role of PriB in primosome assembly based on the ϕX174 system (Sandler et al., 1999). As possible reconciliation of this discrepancy, Sandler et al. reported that a *priBC* double mutant has poor viability and a slowed growth rate, akin to *priA* mutants. Similar to *priB* mutants, mutations that disrupt only *priC* result in near wild-type phenotypes. This raises the possibility that PriB and PriC share redundant functions in the replication restart primosome (Sandler et al., 1999). However, biochemical or structural redundancy between PriB and PriC have not been demonstrated to date.

In this report, we examine the physical basis for PriB function in primosome-mediated replication restart. We purified and crystallized a recombinant form of full-length *E. coli* PriB and determined its structure to 2.0 Å resolution by X-ray diffraction. The structure shows that PriB forms a homodimeric β-barrel with two oligonucleotide/oligosaccharide binding (OB) folds. Each monomer contributes one OB-fold in the PriB dimer. Based on comparison of the structure of PriB with that of *E. coli* SSB, we have identified a surface of PriB that is predicted to play a role in binding ssDNA. Furthermore, we have demonstrated using mutational analysis that several aromatic and basic residues on this surface of PriB directly contribute to ssDNA binding. The structure of PriB also reveals a possible protein interaction surface to which the primosome assembly activity of PriB might be attributed. This is the first high-resolution structure of any of the proteins involved in *oriC*-independent replisome loading and provides unique insight into a critical aspect of genome maintenance in *E. coli*.

Results and Discussion

Structure of *E. coli* PriB Protein

We crystallized a selenomethionine-incorporated variant of the full-length *E. coli* PriB protein and determined its structure to 2.0 Å resolution. Multiwavelength-anomalous dispersion (MAD) phasing techniques were used to generate an electron-density map that was readily interpretable (Figure 1B). The asymmetric unit contains two molecules in a homodimeric arrangement: the model for the first molecule (chain A) includes amino acid residues 1–100 (of 104 total residues), excluding residues 81–88, and the second (chain B) includes amino acid residues 1–98, excluding residues 19–24 and 82–89 (Figure 1). Electron density was not observed for excluded residues, likely reflecting the dynamic nature of these

Table 1. Data Collection, Phasing, and Refinement

Data Collection	Anomalous Peak	Inflection	Remote	Phasing Statistics		Refinement	
Wavelength (Å)	0.9797	0.9798	1.0200	Resolution (Å)	34–2.0	Resolution (Å)	20.0–2.0
Resolution (Å) (last shell Å)	34–2.0 (2.1–2.0)	34–2.0 (2.1–2.0)	34–2.0 (2.1–2.0)	Figure of merit	0.276	R_{work}/R_{free} [b]	25.9/28.5
Multiplicity (last shell)	11.7 (10.1)	7.8 (6.8)	7.5 (5.5)	(after density modification)	0.737	RMSD (°) bond lengths	0.012
Completeness (%) (last shell)	99.7 (99.8)	99.6 (99.8)	98.8 (95.5)			RMSD (Å) bond angles	1.15
R_{sym} (%)[a] (last shell)	12.8 (58.7)	10.1 (58.0)	9.3 (44.7)			Ramachandran statistics	
I/σ (last shell)	14.2 (5.1)	13.6 (4.9)	13.9 (4.6)			% core region	93.3
						% allowed region	6.7
						% generously or disallowed regions	0.0

[a] $R_{sym} = \Sigma\Sigma_j|I_j - <I>|/\Sigma I_j$, where I_j is the intensity measurement for reflection j and $<I>$ is the mean intensity for multiply recorded reflections.
[b] $R_{work/free} = \Sigma||F_{obs}| - |F_{calc}||/|F_{obs}|$, where the working and free R factors are calculated using the working and free reflection sets, respectively. The free reflections (5% of the total) where held aside throughout refinement.

elements of the PriB structure. The structure was refined to a final R-factor of 0.259 (R_{free} 0.285) with good bond geometries. No residues fall into disallowed regions of Ramachandran space (Table 1).

The *E. coli* PriB dimer comprises a single structural domain characterized by a β-barrel from which four prominent β-hairpins extend (Figures 1 and 2). The β-barrel is flanked by α helices that connect the β3 and β4 strands in each monomer. Collectively, these secondary structural elements are organized into two OB-folds, one contributed by each monomer of the PriB dimer (Figure 1C). The core of the β-barrel is formed on one side by two antiparallel β sheets, one from each molecule of PriB in the dimer, that combine to produce an extended, six-stranded β sheet. The opposite side of the β-barrel is also formed by two antiparallel β sheets, but this face of the β-barrel does not form a continuous, extended β sheet as the individual β sheets are separated by the L_{45} loops. The bases of the L_{45} loops extend outward approximately perpendicular to the plane of the β-barrel (Figure 1C, upper). As described above, the distal residues of these loops are absent from the PriB model due to lack of interpretable electron density. In contrast, the L_{23} loops are well defined in the PriB electron density. Although they connect the β2 and β3 strands, whose ends project away from the β-barrel, these loops fold back along the core of the protein, lying nearly parallel to the long axis of the β-barrel (Figure 1C, lower).

While the core of the β-barrel is dominated primarily by hydrophobic residues, the two major surfaces of the β-barrel show a distinct polarity in the abundance of charged residues (Figure 3B). The surface of the PriB dimer corresponding to the continuous six-stranded β sheet contains ten of the twelve glutamate residues and all four aspartate residues, resulting in a net negative charge on this surface of the β-barrel. In contrast, the opposite surface and the sides of the β-barrel contain ten of the twelve arginine residues and all eight lysine residues (Lys82 and Lys84 of both chains, and Lys89 of chain B are located in the L_{45} loops and are absent from the model), resulting in a net positive charge on this surface of the β-barrel.

Dimerization of PriB

In the crystal structure of PriB, the dimerization interface is extensive and intertwined, with portions of one molecule wrapping around the other (Figure 2A). The two molecules comprising the crystallographic asymmetric unit are covalently linked by two disulfide bonds, one between Cys48 of chain A and Cys80 of chain B, and the other between Cys80 of chain A and Cys48 of chain B (Figure 2B). Furthermore, extensive contacts are made through hydrogen bonding between residues 1 through 11 of the N-terminal β1 strands of each molecule in the PriB dimer, bridging the three-stranded β sheets into a single, extended six-stranded β sheet. Additional elements of the dimerization surface are contributed by the L_{23} loops packing against residues in the β3, β4, and β5 strands of the adjacent protomer. This interface involves a complex blend of contacts, including van der Waals interaction surfaces and ionic interactions (Figure 2B). Additional dimerization contacts exist at the bases of the L_{45} loops. The total surface area buried upon dimerization is approximately 2700 $Å^2$. Taken together, the characteristics of the dimerization interface suggest that the individual PriB protomers may not be stable structures on their own but would favor dimerization (Nooren and Thornton, 2003).

Biochemical evidence supports the dimeric form of PriB observed in the crystal structure. The relative mobility of PriB through a denaturing polyacrylamide gel under reducing conditions of 100 mM β-mercaptoethanol is approximately 12,000 Da, although a fraction of the protein migrates at approximately 24,000 Da (data not shown). Under oxidizing conditions, the ratio of the 24,000 Da band relative to the 12,000 Da band increases, suggesting that an equilibrium exists in solution between a dimeric form linked by disulfide bonds and other structures. Mass spectrometry of native PriB and selenomethionine-incorporated PriB revealed that the slower migrating band has a mass of 23,455 Da with six incorporated selenomethionine residues, compared to a mass of 11,728 Da for the faster migrating band with three incorporated selenomethionine residues (data not shown). These mass spectrometry data are consistent with PriB existing in solution as a mixture of covalently

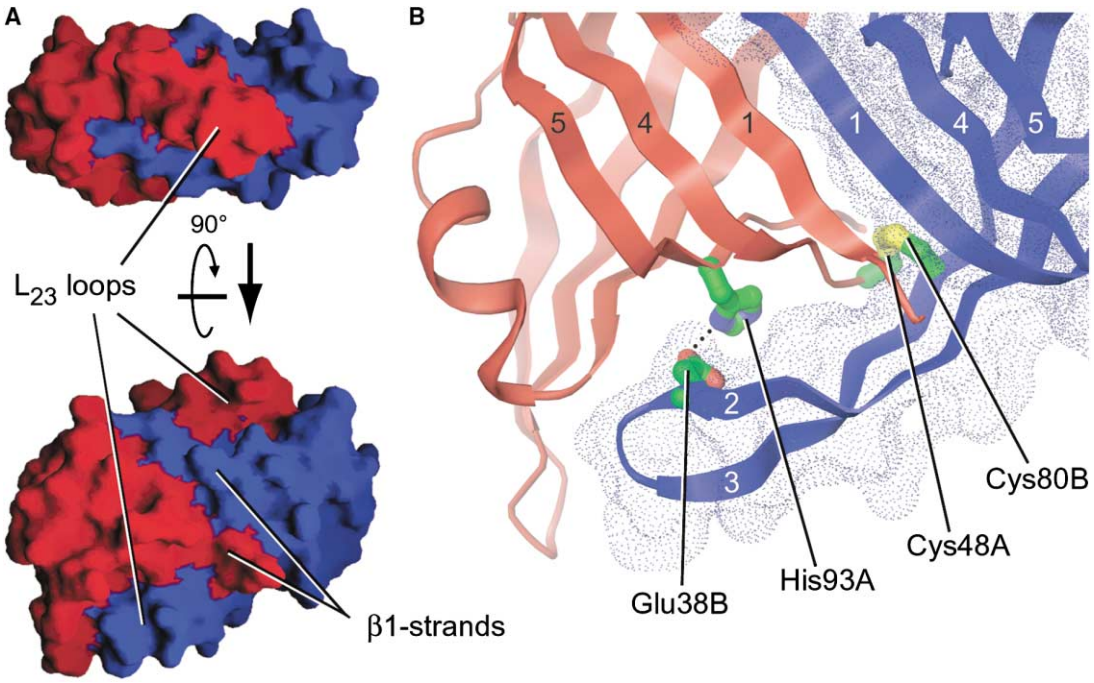

Figure 2. Dimerization Interface of PriB

(A) Orthogonal views of the surface of PriB, colored as in Figure 1. The views are of the same orientation as in Figure 1C and indicate the extensive interdigitization between protomers in the dimer. Surfaces were rendered with the program GRASP (Nicholls et al., 1991).

(B) Close-up view of the dimerization interaction surface involving the L_{23} loop. Individual β strands are numbered as in Figure 1A. Several residues that mediate dimerization are indicated. Ribbons and the surface of chain B are colored as in Figure 1C.

linked dimer and alternate configurations (e.g., noncovalently linked dimer).

Conflicting reports exist on the oligomeric status of PriB. Initial purification and characterization of PriB by Low et al. (1982) indicated that the protein exists as a dimer in solution, although it was determined that only one molecule of PriB is required to form a functional prepriming intermediate on ϕX174 ssDNA. Based on the extensive contacts that comprise the dimerization interface in the PriB crystal structure reported herein, we suggest that the dimeric form of PriB is likely to be the biologically active form of the protein.

Comparison to Single-Stranded DNA Binding Protein

Based on sequence analysis, Ponomarev et al. (2003) concluded that *E. coli* PriB likely arose from SSB by a gene duplication event and later acquired a specialized function in DNA replication. Consistent with this hypothesis, a search of the Protein Data Bank using the program DALI revealed close similarity of the structure of PriB to that of prokaryotic and eukaryotic SSB proteins for which structural information exists, such as *E. coli* SSB (Raghunathan et al., 2000), *D. radiodurans* SSB (Bernstein et al., 2004), human replication protein A (Bochkarev et al., 1999), and human mitochondrial SSB (Yang et al., 1997). PriB and *E. coli* SSB share approximately 11% identity and 27% similarity at the level of amino acid sequence (Figure 1A) and their structures share a number of overall features.

The most prominent similarity of PriB to SSBs is the arrangement of OB-folds. This fold is common to many proteins that bind single-stranded nucleic acids and has been found in a wide range of proteins with seemingly unrelated primary sequence (Murzin, 1993). Specifically, the β-barrel core of PriB is strikingly similar to that of *E. coli* SSB (Figures 1C and 1D). PriB and SSB also share a common dimerization interface, as both proteins employ the N-terminal β1 strand to link adjacent monomers. The loops of PriB, however, show significant differences in both length and conformation compared to those of SSB (Figures 1C and 1D). This is not unexpected, as the length and conformation of loop regions within OB-folds tend to vary among individual proteins depending upon the nature of the substrate to which they bind (reviewed in Theobald et al., 2003). Further differences exist in the extent of multimerization of PriB compared to SSB, an observation that has important implications for the type of protein-protein interactions in which each protein participates (described below). Differences also exist between specific amino acid residues of SSB that are known to play important roles in binding DNA and the analogous residues of PriB. A discussion of the implications of these differences for DNA binding by PriB follows.

Implications for Nucleic Acid Binding

The presence of an SSB-like fold in PriB would seem a reasonable explanation for its observed in vitro ssDNA binding activity (Allen and Kornberg, 1993; Low et al., 1982). However, four highly conserved, key aromatic residues involved in DNA binding by *E. coli* SSB are not

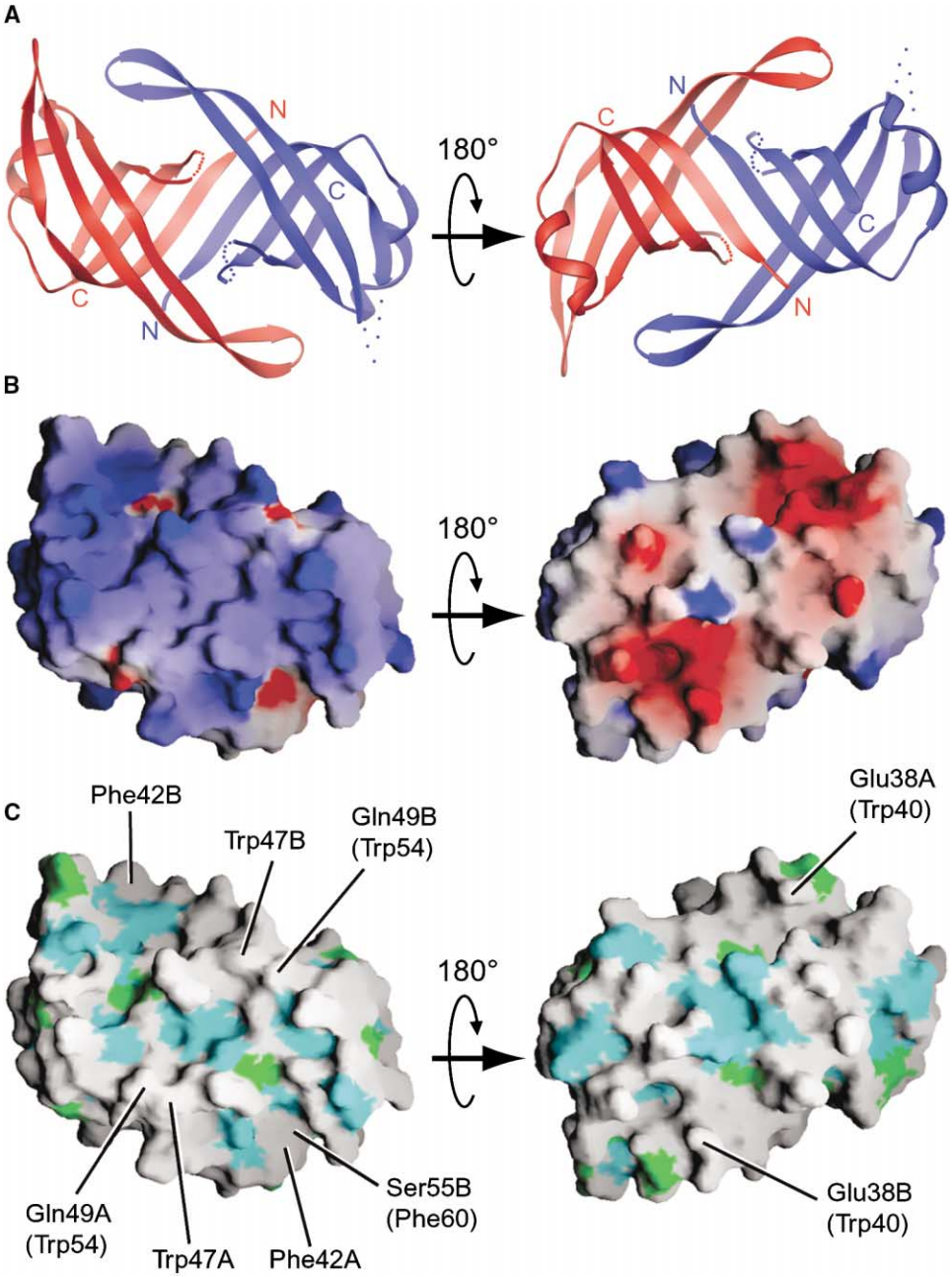

Figure 3. Surface Potential and Residue Conservation of PriB

(A) Ribbon diagram of PriB. The two molecules of PriB are colored as in Figure 1C.

(B) The surface of the PriB dimer is colored by its electrostatic surface potential at ± 6 K_BT/e for positive (blue) or negative (red) charge potential.

(C) The surface of the PriB dimer is colored as in Figure 1A by its conservation with *E. coli* SSB. PriB residues present at positions of three key aromatic residues of *E. coli* SSB are indicated with the equivalent SSB residues in parentheses. Also indicated are surface exposed aromatic residues Phe42 and Trp47 of PriB. (A), (B), and (C) represent the same orientation of PriB.

conserved in the OB-folds of PriB, raising the question of how PriB binds DNA. The crystal structure of *E. coli* SSB with bound oligonucleotides indicates that the aromatic side chains of residues Trp40, Trp54, Phe60, and Trp88 make critical contacts with ssDNA through base stacking interactions (Raghunathan et al., 2000). The analogous residues of PriB, based on their position in the structure, are Glu38, Gln49, and Ser55, respectively, while a structurally analogous residue of SSB Trp88 could not be identified in PriB as it lies within the disordered L_{45} loop (Figure 3C). It is notable, however, that no aromatic residues exist within the L_{45} loop of PriB, so the residue that is a positional equivalent of SSB Trp88 is not likely to play a role in base stacking interactions with DNA. Thus, aromatic base-stacking residues that are structurally homologous to those found in *E. coli*

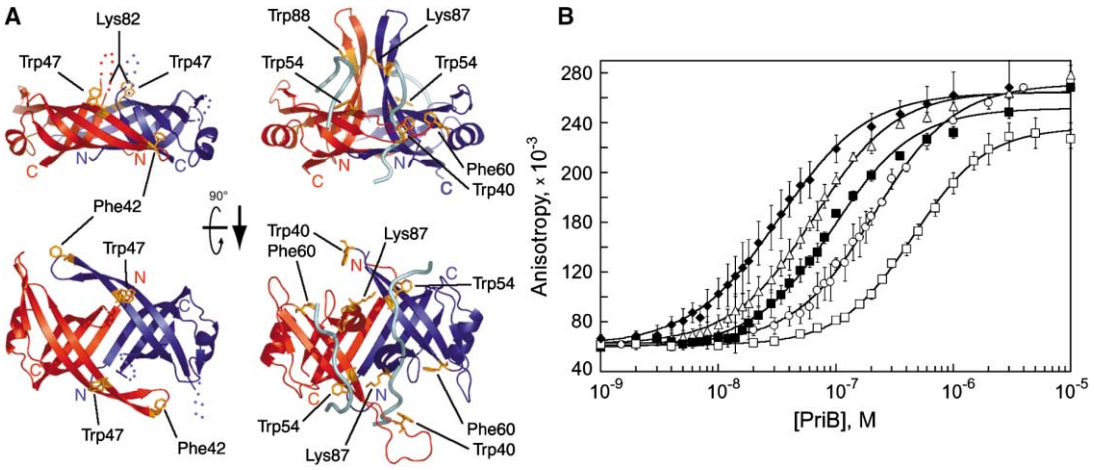

Figure 4. ssDNA Binding by PriB

(A) Orthogonal views of ribbon diagrams of the crystal structures of PriB and SSB. Chains are colored as in Figure 1C and D. Single-stranded DNA oligonucleotide is colored cyan in the SSB ribbon diagram. Residues of PriB and SSB involved in ssDNA binding are represented as stick models and are colored orange. Note that PriB residue Lys82, located at the base of the L_{45} loop, is absent from the model and its labeled position is an approximation. Ribbon diagrams were rendered with the program PyMol (DeLano, 2002).

(B) Wild-type PriB (closed diamonds); F42A (open triangles); W47A (closed squares); K82A (open circles); and W47A,K82A (open squares) were serially diluted and incubated with a fluorescein-conjugated ssDNA oligonucleotide as described in Experimental Procedures. Apparent dissociation constants were calculated by converting anisotropy values to fraction ssDNA bound as a function of PriB concentration. Measurements are reported in triplicate and error bars represent standard deviations of the mean.

SSB are not found in PriB. However, alignment of the structures of both proteins revealed that Trp47 of PriB is positioned approximately 3 Å from the analogous position of Trp54 in SSB (Figure 3C left, and Figure 4A). Close proximity of PriB Trp47 to the position of residue Trp54 of SSB suggests that PriB Trp47 may play a role in nucleic acid binding. In addition, Trp47 is highly conserved among sequenced bacterial PriB homologs, further supporting a role for this residue in the function of PriB (Figure 1A). One additional aromatic residue of PriB is found at the surface of the protein, Phe42 (Figure 3C left). While not conserved with an aromatic residue of SSB involved in DNA binding, PriB Phe42 is located on the same side of the β-barrel that binds DNA in SSB and is near the position of Phe60 in SSB from the adjacent protomer, suggesting that PriB Phe42 could be involved in DNA binding (Figure 4A). Of the remaining aromatic residues of PriB, Phe29 and Phe77, neither is surface exposed and is not likely involved in binding DNA.

To test the role of PriB Trp47 and Phe42 in ssDNA binding, we constructed mutants in which these residues are substituted for alanine. Using fluorescence anisotropy to measure binding of these mutant PriB proteins to a 30-base, fluorescently labeled ssDNA oligonucleotide, we observed that the Trp47 and Phe42 alanine-substitution mutants are defective in binding ssDNA compared to wild-type PriB (Figure 4B). While wild-type PriB bound the ssDNA oligonucleotide with an apparent Kd of 34.6 ± 7.7 nM, the Trp47 and Phe42 mutants showed apparent Kd values of 112.3 ± 7.2 nM and 72.8 ± 11.5 nM, respectively (Table 2). Both mutants appear to be correctly folded based on measurements of secondary structure by circular dichroism spectroscopy (data not shown). These data support a role for aromatic residues Trp47 and Phe42 in ssDNA binding by PriB.

In addition to aromatic base stacking interactions, structural and biochemical studies with *E. coli* SSB demonstrated the importance of electrostatic interactions for ssDNA binding. Specifically, residues Lys43, Lys62, Lys73, and Lys87 show reduced accessibility to chemical modification upon ssDNA binding and are within contact distance of the nucleotide backbone in the structure of the *E. coli* SSB:DNA complex (Chen et al., 1998; Raghunathan et al., 2000). Similar to what is observed for *E. coli* SSB, the putative DNA binding pocket of the PriB OB-fold is strikingly electropositive (Figure 3B left). Interestingly, of the eight lysine residues of the PriB dimer, only Lys82 is positionally conserved with a lysine residue of SSB involved in contacting nucleic acid, Lys87. Located at the base of the L_{45} loop, PriB Lys82 appears to be in a prime position to make contacts with ssDNA (Figure 4A).

To ascertain whether Lys82 plays a role in ssDNA binding, we constructed a mutated version of PriB in which this residue is substituted for alanine and tested the ability of this mutant PriB protein to bind ssDNA using fluorescence anisotropy as described above. Compared with wild-type PriB, the Lys82 alanine-substitution mutant showed a significant defect in ssDNA binding (Figure 4B). The apparent Kd of the Lys82 mutant for the 30-base ssDNA oligonucleotide is 218.2 ± 9.4 nM, a defect greater than 6-fold compared to wild-type PriB

Table 2. ssDNA Binding Constants for PriB Variants

PriB Variant	Apparent Kd, nM
wild type	34.6 ± 7.7
F42A	72.8 ± 11.5
W47A	112.3 ± 7.2
K82A	218.2 ± 9.4
W47A,K82A	426.6 ± 52.3

(Table 2). Combined with the Trp47 alanine-substitution mutation, the defect in ssDNA binding of the Lys82 alanine-substitution mutation is exacerbated, with an apparent Kd of 426.6 ± 52.3 nM for the Trp47/Lys82 double mutant (Figure 4B and Table 2). Similar to the Trp47 and Phe42 mutants, both the Lys82 single mutant and the Trp47/Lys82 double mutant appear to be correctly folded based on measurements of secondary structure by circular dichroism spectroscopy (data not shown). These data support a critical role for PriB Lys82 in ssDNA binding.

Two additional lysine residues reside within the L_{45} loop of PriB, Lys84 and Lys89. We speculate that these residues, like Lys82, might also play an important role in binding ssDNA. While it is not clear if the remaining electropositive residues of PriB play a role in ssDNA binding, the localization of all eight lysine residues of the PriB dimer, as well as Trp47 and Phe42, to the region corresponding to the classic OB-fold ligand binding surface suggests that this face is likely the major site of ssDNA binding by PriB. Taken together, it appears that PriB binds ssDNA on the same general surface of its OB-folds as *E. coli* SSB, although this surface has likely been adapted to bind DNA in a different manner compared to SSB. This feature may reflect one of the ways in which PriB has attained a specialized role in DNA replication.

Implications for Protein Binding

E. coli PriB significantly differs from SSB in its quaternary structure. To date, all known bacterial SSB proteins assemble four OB-folds in their active state. In most bacteria, including *E. coli*, SSB forms homotetramers with each monomer contributing a single OB-fold (Raghunathan et al., 2000). Variations on this theme exist in the *Deinococcus-Thermus* group of bacteria in which SSB proteins form homodimers. In these cases, however, each monomer possesses two OB-folds, resulting in assembly of four OB-folds upon dimerization (Eggington et al., 2004). Unlike SSB, *E. coli* PriB is homodimeric and has two OB-folds. Since it does not appear that the PriB dimer forms higher order oligomers, an important consequence of this arrangement is exposure of a large surface area on one side of the β-barrel, analogous to an oligomerization interface found in SSBs. It is tantalizing to speculate that this surface serves as a protein interaction surface for PriB as well, but that it has evolved for association with heterologous proteins.

As a component of the *E. coli* replication restart primosome that is important for primosome assembly and activity, PriB is thought to interact with several other primosome proteins. Specifically, PriB is thought to bind directly to PriA at a repaired replication fork or D-loop DNA structure and may help stabilize the binding of PriA at the site of primosome assembly (Ng and Marians, 1996). Upon formation of the DNA:PriA:PriB complex, DnaT is recruited into the preprimosomal complex, facilitated by interactions with PriB (Liu et al., 1996). While it is not readily apparent which regions of PriB participate in these protein-protein interactions with PriA and DnaT, our results suggest that the electronegative, continuous six-stranded β sheet that forms a major surface of the β-barrel is an attractive candidate.

In this report, we have described the crystal structure of the *E. coli* PriB homodimer. Based on structural similarity of PriB to single-stranded DNA binding proteins and on mutational analysis, we have identified surface residues of PriB that are involved in ssDNA binding as well as a potential protein interaction surface. We hypothesize that DNA binding by PriB may have become specialized for specific DNA structures that exist at repaired replication forks. Furthermore, the potential protein interaction surface of PriB may be involved in its primosome assembly function by binding PriA and DnaT. Thus, the OB-folds of the PriB dimer probably represent modular but integral components of the larger assembly of proteins that comprise the intact primosome. Further investigation will be required to determine the nature of the physical interaction between PriB and other primosome proteins such as PriA and DnaT, and to address the functional role of ssDNA binding by PriB in the replication restart primosome. Taken together, these features provide new insights into the physical basis for PriB function in origin-independent replisome loading in *E. coli* replication restart pathways.

Experimental Procedures

Molecular Cloning of *priB* and *priB* Mutants

The *priB* gene of *E. coli* was amplified from strain K12 genomic DNA by polymerase chain reaction (PCR) using primers oML102 (5′-GCG TAT TCC ATA TGA CCA ACC GTC TGG TGT TGT CC) and oML103 (5′-GTC ACG GAT CCC TAG TCT CCA GAA TCT ATC AA). The PCR-amplified product was cloned into the pET28.b expression vector (Novagen) using NdeI and BamHI restriction sites. The resulting plasmid, pML101, contains sequence coding for a six-histidine tag and thrombin cleavage site fused to the 5′ end of *priB*. The recombinant *priB* gene is under the control of a T7 promoter for overexpression in hosts harboring T7 polymerase controlled by the *lacUV5* promoter. Plasmid pML101 was transformed into BL21(DE3) *E. coli* to allow recombinant PriB protein overexpression following induction with isopropyl-β-D-thiogalactopyranoside (IPTG). Mutant *priB* genes were constructed using the QuikChange site-directed mutagenesis kit (Stratagene) according to the manufacturer's instructions. Mutant F42A was generated with primers oML111 (5′-GTG CAG GAG GAA GCC GGC GCT CAC CGG CAG GCG TGG TG) and oML112 (5′-CAC CAC GCC TGC CGG TGA GCG CCG GCT TCC TCC TGC AC). Mutant W47A was generated with primers oML117 (5′-GGC TTT CAC CGG CAG GCG GCG TGT CAA ATG CCC GTT AT) and oML118 (5′-ATA ACG GGC ATT TGA CAC GCC GCC TGC CGG TGA AAG CC). Mutant K82A was generated with primers oML115 (5′-GGG TTC ATT TCA TGC CAC GCG GCA AAG AAC GGA CTG AG) and oML116 (5′-CTC AGT CCG TTC TTT GCC GCG TGG CAT GAA ATG AAC CC). Double-mutant W47A,K82A was generated with primers oML117 and oML118 in the context of the previously constructed K82A mutation. The fidelity of wild-type and mutant *priB* genes was confirmed by DNA sequencing.

Purification of PriB Proteins

Cultures of BL21(DE3) *E. coli* harboring plasmid pML101 were grown in minimal medium containing 52 $\mu g \cdot mL^{-1}$ selenomethionine and 50 $\mu g \cdot mL^{-1}$ kanamycin at 37°C to an OD_{600} of 0.6. IPTG was added to 1 mM and growth was continued for 4 hr. Cells were harvested by centrifugation at 5,000 × *g* and lysed in 20 mM Tris·HCl (pH 7), 1 M NaCl, 10 mM imidazole, 1 mM Tris(2-carboxyethyl)phosphine hydrochloride (TCEP), and 1 mM phenylmethylsulfonyl fluoride (PMSF) by sonication on ice. Lysates were clarified by centrifugation at 26,000 × *g* and His-tagged PriB was bound to nickel-NTA agarose (Qiagen). The nickel-NTA agarose beads were washed with lysis buffer and bound proteins were eluted in 20 mM Tris·HCl (pH 7), 1 M NaCl, 250 mM imidazole, and 1 mM TCEP. The nickel-NTA agarose eluant was dialyzed against 20 mM Tris·HCl (pH 7), 0.3 M NaCl, and

digested with thrombin to remove the His-tag, leaving a Gly-Ser-His sequence at the amino-terminus directly preceding the first methionine residue. Residual His-tagged PriB that was not cleaved by thrombin, as well as contaminating *E. coli* proteins, were depleted with nickel-NTA agarose. Thrombin-cleaved PriB was concentrated and purified through a Sephacryl S-100 size exclusion column (Pharmacia) in 10 mM Tris·HCl (pH 7), 1 M NaCl, and 1 mM TCEP. PriB fractions were pooled, concentrated to 15 mg·mL^{-1}, and stored at 4°C. For single-stranded DNA binding assays, wild-type PriB and mutant PriB proteins were purified essentially as described above, except that the BL21(DE3) cells were grown in Lauria-Bertani (LB) medium, 1 mM β-mercaptoethanol was used in all buffers in place of TCEP, and the His-tag was not removed.

Crystallization of PriB

PriB was dialyzed against 10 mM Tris·HCl (pH 7), 0.3 M ammonium acetate. Crystals were grown by hanging drop vapor diffusion by mixing 1 μl of 15 mg·mL^{-1} PriB with 1 μl well solution comprising 8% polyethylene glycol (PEG) 8000, 0.1 M Tris·HCl (pH 8.5), and equilibrating at room temperature. Crystals measuring ~100 μm × ~100 μm × ~150 μm of symmetry $P2_12_12_1$ with unit cell dimensions a = 49.8, b = 60.2, c = 66.2 Å, grew over a period of several days. Crystals were stabilized by transferring into cryoprotectant solution comprising 0.1 M Tris·HCl (pH 8.5), 10% PEG 8000, 35% glycerol, 1 mM TCEP, and frozen in liquid nitrogen (McFerrin and Snell, 2002).

MAD Phasing and Model Refinement

The structure of selenomethionine-incorporated PriB was solved to 2.0 Å resolution using MAD phasing (Table 1). Data were indexed and scaled with MOSFLM (Leslie, 1992) and SCALA (Kabsch, 1988) and selenium sites were identified with SOLVE (Terwilliger and Berendzen, 1999) and further refined with MLPHARE (Otwinowski, 1991). Solvent flattening with DM (Cowtan, 1994) resulted in interpretable electron-density maps for model building. These steps were performed automatically using ELVES (Holton and Alber, 2004). Part of the model was built automatically with ARP/wARP (Lamzin and Wilson, 1993) and the remainder was built manually with the program O (Jones et al., 1991). The model was improved by multiple rounds of refinement with REFMAC5 (Winn et al., 2001).

Single-Stranded DNA Binding Assay

PriB proteins were diluted serially from 10,000 nM to 0.01 nM into 20 mM Tris·HCl (pH 8), 50 mM NaCl, 4% glycerol, 1 mM $MgCl_2$, 1 mM β-mercaptoethanol, and 0.1 mg·mL^{-1} bovine serum albumin. Dilutions of PriB proteins were incubated at room temperature with 1 nM 3′-fluorescein-conjugated single-stranded DNA oligonucleotide (5′-GCG TGG GTA ATT GTG CTT CAA TGG ACT GAC) in a total volume of 100 μl for 30 min. The anisotropy of each sample was measured at 25°C with a Beacon 2000 fluorescence polarization system. Anisotropy data are reported in triplicate and error bars represent standard deviations of the mean. Apparent Kd values of PriB proteins for the 30-base ssDNA oligonucleotide were derived from anisotropy data converted into the fraction of ssDNA bound as a function of PriB concentration. Uncertainties reported with apparent Kd values are standard deviations of the mean.

Acknowledgments

This work was supported by a grant from the Shaw Foundation for Medical Research and National Institutes of Health grant GM068061 to J.L.K. X-ray diffraction data were collected at the Advanced Light Source Beamline 8.3.1. We thank Darrell R. McCaslin of the University of Wisconsin-Madison Biophysics Instrumentation Facility, which is supported by the University of Wisconsin-Madison, National Science Foundation grant BIR-9512577, and National Institutes of Health grant S10 RR13790, for assistance with circular dichroism spectroscopy. We are also grateful to Steven Sandler and members of the Keck lab for critical review of the manuscript.

Received: July 7, 2004
Revised: September 20, 2004
Accepted: September 21, 2004
Published online: September 30, 2004

References

Allen, G.C., Jr., and Kornberg, A. (1993). Assembly of the primosome of DNA replication in Escherichia coli. J. Biol. Chem. *268*, 19204–19209.

Bernstein, D.A., Eggington, J.M., Killoran, M.P., Misic, A.M., Cox, M.M., and Keck, J.L. (2004). Crystal structure of the *Deinococcus radiodurans* single-stranded DNA-binding protein suggests a mechanism for coping with DNA damage. Proc. Natl. Acad. Sci. USA *101*, 8575–8580.

Bochkarev, A., Bochkareva, E., Frappier, L., and Edwards, A.M. (1999). The crystal structure of the complex of replication protein A subunits RPA32 and RPA14 reveals a mechanism for single-stranded DNA binding. EMBO J. *18*, 4498–4504.

Carson, M. (1997). Ribbons. Methods Enzymol. *277*, 493–505.

Chen, J., Smith, D.L., and Griep, M.A. (1998). The role of the 6 lysines and the terminal amine of Escherichia coli single-strand binding protein in its binding of single-stranded DNA. Protein Sci. *7*, 1781–1788.

Cowtan, K. (1994). Joint CCP4 and ESF-EAMCB Newsletter on Protein Crystallography *31*, 34–38.

Cox, M.M., Goodman, M.F., Kreuzer, K.N., Sherratt, D.J., Sandler, S.J., and Marians, K.J. (2000). The importance of repairing stalled replication forks. Nature *404*, 37–41.

DeLano, W.L. (2002). The PyMOL Molecular Graphics System. (San Carlos, CA: DeLano Scientific).

Eggington, J.M., Haruta, N., Wood, E.A., and Cox, M.M. (2004). The single-stranded DNA-binding protein of Deinococcus radiodurans. BMC Microbiol. *4*, 2.

Holton, J., and Alber, T. (2004). Automated protein crystal structure determination using ELVES. Proc. Natl. Acad. Sci. USA *101*, 1537–1542.

Jones, T.A., Zou, J.Y., Cowan, S.W., and Kjeldgaard, G. (1991). Improved methods for building protein models in electron density maps and the location of errors in these models. Acta Crystallogr. A *47*, 110–119.

Kabsch, W. (1988). Evaluation of single-crystal X-ray diffraction data from a position-sensitive detector. J. Appl. Crystallogr. *21*, 916–924.

Kaguni, J.M., and Kornberg, A. (1984). Replication initiated at the origin (oriC) of the E. coli chromosome reconstituted with purified enzymes. Cell *38*, 183–190.

Lamzin, V.S., and Wilson, K.S. (1993). Automated refinement of protein models. Acta Crystallogr. D Biol. Crystallogr. *49*, 129–147.

Leslie, A.G.W. (1992). Recent changes to the MOSFLM package for processing film and image plate data. Joint CCP4 and ESF EAMCB Newsletter on Protein Crystallography *26*.

Liu, J., Nurse, P., and Marians, K.J. (1996). The ordered assembly of the phiX174-type primosome. III. PriB facilitates complex formation between PriA and DnaT. J. Biol. Chem. *271*, 15656–15661.

Liu, J., and Marians, K.J. (1999). PriA-directed assembly of a primosome on D loop DNA. J. Biol. Chem. *274*, 25033–25041.

Low, R.L., Shlomai, J., and Kornberg, A. (1982). Protein n, a primosomal DNA replication protein of Escherichia coli. Purification and characterization. J. Biol. Chem. *257*, 6242–6250.

McFerrin, M.B., and Snell, E.H. (2002). The development and application of a method to quantify the quality of cryoprotectant solutions using standard area-detector X-ray images. J. Appl. Crystallogr. *35*, 538–545.

Murzin, A.G. (1993). OB(oligonucleotide/oligosaccharide binding)-fold: common structural and functional solution for non-homologous sequences. EMBO J. *12*, 861–867.

Ng, J.Y., and Marians, K.J. (1996). The ordered assembly of the phiX174-type primosome. I. Isolation and identification of intermediate protein-DNA complexes. J. Biol. Chem. *271*, 15642–15648.

Nicholls, A., Sharp, K.A., and Honig, B. (1991). Protein folding and association: insights from the interfacial and thermodynamic properties of hydrocarbons. Proteins *11*, 281–296.

Nooren, I.M., and Thornton, J.M. (2003). Diversity of protein-protein interactions. EMBO J. *22*, 3486–3492.

Otwinowski, Z. (1991). Maximum likelihood refinement of heavy atom parameters. Proceedings of the CCP4 Study Weekend, 80–86.

Ponomarev, V.A., Makarova, K.S., Aravind, L., and Koonin, E.V. (2003). Gene duplication with displacement and rearrangement: origin of the bacterial replication protein PriB from the single-stranded DNA-binding protein Ssb. J. Mol. Microbiol. Biotechnol. *5*, 225–229.

Raghunathan, S., Kozlov, A.G., Lohman, T.M., and Waksman, G. (2000). Structure of the DNA binding domain of E. coli SSB bound to ssDNA. Nat. Struct. Biol. *7*, 648–652.

Sandler, S.J., Marians, K.J., Zavitz, K.H., Coutu, J., Parent, M.A., and Clark, A.J. (1999). dnaC mutations suppress defects in DNA replication- and recombination-associated functions in priB and priC double mutants in Escherichia coli K-12. Mol. Microbiol. *34*, 91–101.

Sandler, S.J., and Marians, K.J. (2000). Role of PriA in replication fork reactivation in Escherichia coli. J. Bacteriol. *182*, 9–13.

Schekman, R., Weiner, J.H., Weiner, A., and Kornberg, A. (1975). Ten proteins required for conversion of phiX174 single-stranded DNA to duplex form in vitro. Resolution and reconstitution. J. Biol. Chem. *250*, 5859–5865.

Terwilliger, T.C., and Berendzen, J. (1999). Automated MAD and MIR structure solution. Acta Crystallogr. D Biol. Crystallogr. *55*, 849–861.

Theobald, D.L., Mitton-Fry, R.M., and Wuttke, D.S. (2003). Nucleic acid recognition by OB-fold proteins. Annu. Rev. Biophys. Biomol. Struct. *32*, 115–133.

Wickner, S., and Hurwitz, J. (1974). Conversion of phiX174 viral DNA to double-stranded form by purified Escherichia coli proteins. Proc. Natl. Acad. Sci. USA *71*, 4120–4124.

Winn, M.D., Isupov, M.N., and Murshudov, G.N. (2001). Use of TLS parameters to model anisotropic displacements in macromolecular refinement. Acta Crystallogr. D Biol. Crystallogr. *57*, 122–133.

Yang, C., Curth, U., Urbanke, C., and Kang, C. (1997). Crystal structure of human mitochondrial single-stranded DNA binding protein at 2.4 A resolution. Nat. Struct. Biol. *4*, 153–157.

Zavitz, K.H., DiGate, R.J., and Marians, K.J. (1991). The priB and priC replication proteins of Escherichia coli. Genes, DNA sequence, overexpression, and purification. J. Biol. Chem. *266*, 13988–13995.

Accession Numbers

Coordinates and structure factors have been deposited in the Protein Data Bank (accession code 1TXY).